Society For Biomaterials

Two-photon confocal imaging study: Cell uptake of two photon dyes-labeled PAMAM dendrons in HeLa cells

Hsieh-Chih Tsai,[1] Toyoko Imae,[1,2] Gabriela Calderó,[3] Conxita Solans[3]

[1]Graduate Institute of Applied Science and Technology, National Taiwan University of Science and Technology, Taipei 10607, Taiwan, Republic of China

[2]Department of Chemical Engineering, National Taiwan University of Science and Technology, Taipei 10607, Taiwan, Republic of China

[3]Institute for Advanced Chemistry of Catalonia (IQAC/CSIC), CIBER-BBN, C/Jorge Girona Salgado, 18–26, Barcelona 08034, Spain

Received 15 August 2011; revised 14 September 2011; accepted 26 September 2011
Published online 11 January 2012 in Wiley Online Library (wileyonlinelibrary.com). DOI: 10.1002/jbm.a.33283

Abstract: A two-photon excitation difluoroboron dye activated in the near infrared region for biological image analysis was synthesized in this study. Cell affinity, membrane interaction, and the endocytosis pathway of PAMAM dendrons were investigated using only covalent two-photon dyes (TPD) at the periphery of the PAMAM dendrons. Generation 3 TPD-labeled PAMAM dendrons (BG3) exhibited multivalency binding on the HeLa cell membranes from the cell affinity study in the fixation of HeLa cells. Photo-stimulation on the membrane of the living HeLa cell was observed by confocal optical imaging *in situ*, using the two-photon model, when incubated with BG3. Analyses of cell membrane integrity via lactate dehydrogenase (LDH) assay confirmed membrane damage at two photon excitation model. However, no variation in the cell was observed using the one-photon excitation model. These results indicated a high degree of dendrons uptake by cells through binding to the cell membrane following the endocytotic pathway. Furthermore, the wide excitation fluorescence spectrum of difluoroboron dye provides dual imaging with which to study the endocytosis of TPD-labeled PAMAM dendrons using a single near infrared laser. J Biomed Mater Res Part A: 100A: 746–756, 2012.

Key Words: two photo confocal microscopy, PAMAM dendron, cell membrane interaction, macromolecular probe

How to cite this article: Tsai H-C, Imae T, Calderó G, Solans C. 2012. Two-photon confocal imaging study: Cell uptake of two photon dyes-labeled PAMAM dendrons in HeLa cells. J Biomed Mater Res Part A 2012:100A:746–756.

INTRODUCTION

Two-photon excitation techniques are related to novel imaging in cell biology. Lasers used to excite two-photon fluorescence lie in the near infrared region (700–1000 nm), and two-photon excitation from laser light provides deeper penetration into the living tissue. The process of two-photon absorption takes place only in the focus of the laser beam, thereby providing three dimensional resolutions. Similarly, phototoxicity from two-photon absorption occurs only at the focal point. The other benefit of two-photon excitation is the application of dual color labeling for cell imaging. Dual or multi-color optical images of cells are common in confocal microscopy for the identification of individual cell organisms or to determine the trace of drug carrier uptake in the cell. However, most two-photon confocal microscopes are fitted with only a single expensive, femtosecond laser. The difficulty stems from the fact that single excitation wavelengths rarely show well separated fluorescence unmixing of overlapping emission profiles.

The discovery of multi-photon dyes exhibiting long-range excitation wavelength is important. One multi-photon dye, a difluoroboron-based dye, such as BODIPY and β-diketonate derivative, exhibiting high emission quantum yields,[1,2] two large photon absorption cross sections,[3] and a wide range near infrared region,[4] could be designed and synthesized for the above mentioned approach. This long-range excitation wavelength from the multi-photon absorption process would be a useful tool for identifying color in cell imaging research. Therefore, this study uses a single excitation wavelength to identify the trace or drug carrier localization with separated excitation wavelengths.

Dendrimers are widely used in pharmaceutical applications, for example, carrying drugs and genes to specific cells, and its architecture can dramatically influence pharmacokinetics. Internalizing a therapeutic agent into the void space within the periphery and core, or attachment by covalent bonding to a functional surface group, is one such application. Most research on dendritic polymers has focused on globular dendrimes with a point core; however, recent work

Additional Supporting Information may be found in the online version of this article.

Correspondence to: H.-C. Tsai; e-mail: h.c.tsai@mail.ntust.edu.tw or T. Imae; e-mail: imae@mail.ntust.edu.tw

has involved preparation and study of dendritic molecules. Hyperbranched polymers are another class of dendritic polymer receiving considerable attention due to their dendrimer-like properties.[5,6] Dendrons, also called dendritic molecules, are typically asymmetric partial dendrimers and can be fabricated either covalently or non-covalently in complete dendritic polymers. Dendrons self-assembly could also lead to vesicular structure of the dendrisome[7] and a covalent dendron structure in the linear polymer to construct a dendritic polymer.[8–11] The dendron structure plays an important role in the aforementioned structures.

Several mechanisms have been proposed to describe molecular transport across cell membranes, such as endocytosis, passive diffusion, carrier-mediated, and paracellular transport. However, dendritic polymer have been widely investigated as carrier to overcome the intracellular barrier via either paracellular or transcellular pathways.[12] Previous studies have reported that the shape or generation of the dendrimer may play a role in forming dendrimer-lipid complexes on the membrane.[13–15] Dendrimer cell membrane interaction has been directly observed by using atomic force microscopy and fluorescence microscopy.[16–18] In addition, Dendrimer have been reported exhibited higher binding affinity on cell membrane also called as multivalency effect[19] and therefore induced the nano-holes formation or expanded the size of pre-existing defects in the lipid bilayer.[16,17] However, limited knowledge of the influence of dendrons on membrane transport and cellular uptake has restricted progress toward biomedical application such as drug delivery design and biomaterials and cell membrane interaction. The current research synthesized a difluoroboron based dye, excited by multiple photons in the near infrared region, and then conjugated it with three-generation PAMAM dendrons (BG1, BG2, and BG3). This work also investigated the cell affinity of BG1, BG2, and BG3 through exposure to fixed HeLa cells. To observe the endocytosis of high generation BG on HeLa cells, we simultaneously obtained an optical image using one photon and two-photon confocal microscopy. Finally, localization of BG3 was determined using a two-color image of the HeLa cell using a stained lysosome compartment and coexisting BG3. Results from these two photon excitation images provide information to realize the cell uptake process of the TPD-labeled PAMAM dendrons.

EXPERIMENT

Materials

Chemicals such as, methyl acrylate, ethylenediamine, succinic anhydride, 4-dimethylaminopyridine, and boron trifluoride etherate (48% BF_3) were purchased from Acros. *Tert*-butyl 2-aminoethylcarbamate 3-oxo-3-(2-(3-oxo-3-phenylpropanoyl)-phenoxy)propanoic acid, dichrolomethane, and triethylamine were purchased from TCI, Aldrich, Wako, and Alfa. Solvents, methanol and *N*,*N*-dimethylsulfoxide (DMSO), were purchased from Acros. The Lyso Tracker DND-99 and Nile Red were obtained from Molecular Probes. Fetal bovine serum (FBS) was obtained from Perbio. Dulbecco's Modified Eagle Medium (DMEM) and Dulbecco's Phosphate Buffered Saline (PBS) were obtained from Gibco. All products were used as received.

Materials characteristic

Changes in the chemical structure of dendrons and dye molecule were monitored on the basis of ^{1}H NMR and ^{13}C NMR spectra. ^{1}H NMR and ^{13}C NMR were recorded on a Bruker Avance-500 MHz using $CDCl_3$ as solvents and tetramethylsilane (TMS) as an internal standard. Identification of chemical groups was examined by IR spectroscopy using a Fourier Transform IR spectrometer (Nicolet-6700). Investigations were performed in the absorption mode, using KBr pellet techniques, at a resolution of 4 cm^{-1}. A mass spectrum was obtained using a Finnigan/MAT 95XL-T spectrometer. Elemental analyses were performed on a Vario EL elementary analyzer.

Synthesis of TPD-labeled PAMAM dendrons

Synthesis of G0.5, G1.5, and G2.5. A 10 mL methanol solution of core reagent *tert*-butyl 2-aminoethylcarbamate, G1 or G2, was carefully added drop wise to a stirred 10 mL methanol solution of methyl acrylate and furthermore stirred for 48 h under nitrogen at room temperature. The solvent was removed under reduced pressure at 40°C using a rotary evaporator, and the resulting colorless oil was dried under a vacuum overnight to obtain the final product:

G0.5: Yield 96%, transparent liquid, IR cm^{-1}: 1740 (C=O); ^{1}H NMR ($CDCl_3$) δ = 1.438 (s, 9H, $(CH_3)_3$-C), 2.406–2.433 (t, 4H, CH_2COO), 2.499–2.522 (t, 2H, $CH_2N(CH_2)_2$), 2.727–2.753 (t, 4H, CH_2CH_2COO), 3.159–3.169 (m, 2H, CH_2NH), 3.675 (s, 6H, CH_3O), 5.081 (s, 1H, NHCOO). ^{13}C NMR ($CDCl_3$): δ: 28.3, 33.6, 38.7, 39.4, 39.9, 51.5, 54.3, 79.4, 156.2, 174.8. MS: *m/z* Calcd for $C_{15}H_{28}N_2O_6$: 332, Found 333 $(M+H)^+$, Elemental Analysis: Calcd: C, 54.20; H, 8.49; N, 8.43, Found: C, 54.18; H, 8.48; N8.44.

G1.5: Yield 92%, light yellow liquid, IR cm^{-1}: 1740 (C=O); ^{1}H NMR ($CDCl_3$) δ = 1.430 (s, 9H, $(CH_3)_3$-C), 2.342–2.683 (t, 4H, CH_2CONH), 2.425–2.457 (m, 8H, CH_2CH_2COO), 2.545–2.568 (m, 6H, $CH_2N(CH_2)_2$)), 2.751–2.803 (m, 12H, $CH_2CH_2NCH_2$ [near focal point], $CH_2N(CH_2)_2$), 3.185–3.195 (m, 2H, CH_2NH), 3.675 (s, 6H, CH_3O). ^{13}C NMR ($CDCl_3$): δ: 28.2, 33.6, 38.5, 39.4, 39.5, 51.2, 54.7, 79.4, 156.6, 174.6. MS: *m/z* Calcd for $C_{33}H_{60}N_6O_{12}$: 732, Found 734 $(M+2H)^+$, Elemental Analysis: Calcd: C, 54.08; H, 8.25; N, 11.47; Found: C, 54.03; H, 8.27; N,11.36.

G2.5: Yield 94% yellow liquid, IR cm^{-1}: 1740 (C=O); ^{1}H NMR ($CDCl_3$) δ = 1.433 (s, 9H, $(CH_3)_3$-C), 2.346–2.2.371 (t, 4H, CH_2CH_2CONH), 2.431–2.459 (t, 16H, CH_2CH_2CHOO), 2.549–2.596 (m, 14H, $CH_2N(CH_2)$), 2.747–2.833 (m, 28H, CH_2CONH, CH_2COO), 3.182 (t, 2H, $CH_2CH_2NCH_2$ [near focal point]), 3.302–3.309 (m, 12H, $CH_2CH_2NCH_2$), ^{13}C NMR ($CDCl_3$): δ: 28.5, 33.6, 38.4, 39.4, 39.5, 51.6, 54.5, 79.6, 156.5, 174.6. MS: *m/z* Calcd for $C_{69}H_{124}N_{14}O_{24}$: 1532, Found 1533 $(M+H)^+$, Elemental Analysis: Calcd: C, 54.03; H, 8.15; N, 12.78, Found: C, 53.95; H, 8.19; N12.85.

Synthesis of G1, G2, and G3. A 5 mL methanol solution of G0.5, G1.5, or G2.5 was slowly added to a vigorously stirred 10 mL methanol solution of 1,2-diaminoethane. After complete addition, the mixture was continuously stirred for 4 days at room temperature. The solvent was then removed

under reduced pressure, maintaining a temperature lower than 40°C.

G1: Yield 83%, transparent liquid, IR cm^{-1}: 1640 (amide I), 1557 (bending, NH_2) 3300 (NH_2); ^1H NMR ($CDCl_3$) δ = 1.438 (s, 9H, $(CH_3)_3$-C), 2.406–2.433 (t, 4H, CH_2CONH), 2.499–2.522 (m, 6H, $CH_2N(CH_2)_2$,$CH_2CH_2NH_2$), 2.727–2.753 (t, 4H, CH_2CH_2COO), 2.875 (t, 4H, CH_2NH_2), 3.159–3.169 (m, 2H, CH_2CH_2N), 5.081 (s, 1H, NHCOO). ^{13}C NMR ($CDCl_3$): δ: 28.4, 33.5, 38.8, 39.5, 39.8, 54.4, 79.1, 156.1, 174.7. MS: *m/z* Calcd for $C_{17}H_{36}N_6O_4$: 388, Found 388, Elemental Analysis: Calcd: C, 52.56; H, 9.34; N, 24.63; Found: C, 52.49; H, 9.33; N, 24.59.

G2: Yield 87%, light yellow liquid, IR cm^{-1}: 1640 (amide I), 1557 (bending, NH_2), 3300 (NH_2); ^1H NMR ($CDCl_3$) δ = 1.435 (s, 9H, $(CH_3)_3$-C), 2.362–2.433 (m, 12H, CH_2CONH), 2.437–2.455 (m, 12H, CH_2CH_2N, $CH_2CH_2NH_2$), 2.531–2.559 (m, 12H, CH_2CH_2CONH), 2.731–2.738 (m, 6H, $CH_2N(CH_2)_2$), 2.812–2.820 (t, 8H, CH_2NH_2), 3.279–3.312 (m, 10H, CH_2NH_2, $CH_2CH_2N(CH_2)_2$). ^{13}C NMR ($CDCl_3$): δ: 28.2, 33.5, 38.8, 39.4, 39.8, 54.3, 79.2, 156.1, 174.7. MS: *m/z* Calcd for $C_{37}H_{76}N_{14}O_8$: 844, Found 842 $(M-2H)^+$, Elemental Analysis: Calcd: C, 52.59; H, 9.06; N, 23.20; Found: C, 52.48; H, 9.03; N, 23.13.

G3: Yield 90%, yellow liquid, IR cm^{-1}: 1640 (amide I), 1557 (bending, NH_2), 3300 (NH_2); ^1H NMR ($CDCl_3$) δ = 1.548 (s, 9H, $(CH_3)_3$-C), 2.175 (b, 16H, $CH_2CH_2NH_2$), 2.363–2.416 (m, 12H, CH_2CH_2CO), 2.539–2.548 (t, 6H, CH_2CH_2N), 2.737–2.753 (t, 12H, CH_2CH_2CO), 2.808–2.830 (t, 16H, CH_2NH_2), 3.192–3.198 (t, 4H, CH_2CH_2N) 3.249–3.299 (m, 10H, $CH_2CH_2NH_2$ and CH_2CH_2N [Near focal point]). ^{13}C NMR ($CDCl_3$): δ: 28.4, 33.7, 38.9, 39.5, 39.8, 54.7, 79.1, 156.1, 174.9. MS: *m/z* Calcd for $C_{77}H_{156}N_{30}O_{16}$: 1756, Found 1758 $(M+2H)^+$, Elemental Analysis: Calcd: C, 52.60; H, 8.94; N, 23.09, Found: C, 52.58; H, 8.99; N, 23.11.

Synthesis of TPD. Reagents of 3-oxo-3-(2-(3-oxo-3-phenylpropanoyl)phenoxy) propanoic acid (1 g), succinic anhydride (0.5 g), dimethylaminopyridine (0.1 mg), and 1.2 mL triethylamine were dissolved in THF and left overnight at room temperature. The resultant solution was poured into deionized water, and the resulting mixture was extracted three times using dichrolomethane (DCM). The residue solid was purified by column chromatography (DCM/hexane). The pink precipitate, which was obtained by evaporating the solvent, was used for further reaction with 2 mL BF_3Et_2O in CH_2Cl_2 at 60°C for 1 h. The reaction mixture was concentrated by a rotary evaporator under reduced pressure. For further purified the final compound was re-crystallized from acetone and hexane (1:3). Yield 82%, dark yellow solid, IR cm^{-1}: 1644 (C=O, carboxyl), 1631 (C=O, complexified with B), 3400 (—OH), ^1H NMR ($CDCl_3$): 2.688–2.709 (t, 2H, CH_2CH_2COOH), 2.836–2.980 (t, 2H, CH_2COOH), 6.252 (s, 1H, COCHCO), 7.433–7.502 (m, 5H, Ar-H, para to PhCOO(meta to PhCO), ortho to PhCO and meta to PhCOO, para to PhCO and meta to PhCO), 7.743–7.746 (t, 1H, Ar-H, meta to PhCOO and Para to PhCO), 7.911–7.92(d, 1H, Ar-H, ortho to PhCO), 8.186–8.199 (d, 1H, Ar-H, ortho to PhCOO) ^{13}C NMR ($CDCl_3$): δ:43.2, 48.6, 92.3, 121.2, 121.2, 125.2, 127.4, 127.9, 130.5, 136.2, 146.5, 168.0, 169.2, 180.1. MS: *m/z* Calcd for $C_{18}H_{14}B_1F_2O_6$: 375, Found 375, 374, Elemental Analysis: Calcd: C, 57.63; H, 3.76, Found: C, 57.62; H, 3.76.

Synthesis of BG1, BG2, and BG3. A mixture of DMAP (8 mg, 0.06 mmol) and EDC (178 mg, 0.93 mmol) was added to a 5 mL dry DMSO solution of dye TPD (360 mg, 0.93 mmol) and G3 PAMAM dendrons (200 mg, 0.11 mmol) while stirring. The reaction mixture was stirred for 1 day. The precipitate (byproduct) was removed by filtration and the solvent was removed under a reduced pressure. Dendrons materials were purified by dialysis with a 1000 Da cutoff membrane against methanol for 1 day.

BG1: Yield 69%, IR cm^{-1}: 1640 (amide I): 1644 (C=O, carboxyl of TPD), 1631 (C=O, complexified with B), ^1H NMR ($CDCl_3$) δ =1.497 (s, 9H, $(CH_3)_3$-C), 2.259–2.288 (m, 4H, CH_2CH_2COOPh), 2.506–2.522 (m, 8H, CH_2CONH, CH_2COOPh), 2.653–2.702 (m, 6H, $CH_2N(CH_2)_2$,CH_2CH_2NHCO), 2.712–2.721 (t, 4H, CH_2CH_2COO), 3.499 (m, 8H, CH_2CH_2N, CH_2NHCO) 6.854 (s, 2H, COCHCO), 7.446–7.503 (m, 10H, Ar-H, para to PhCOO and meta to PhCO, ortho to PhCO and meta to PhCOO, para to PhCO and meta to PhCO), 7.706–7.708 (t, 2H, Ar-H, meta to PhCOO and para to PhCO), 7.946–7.965 (d, 2H, Ar-H ortho to PhCO), 8.247–8.266 (d, 2H, Ar-H, ortho to PhCOO).

BG2 Yield 72%, IR cm^{-1}: 1642 (C=O), 1644 (C=O, carboxyl of TPD), 1632 (C=O, B complex with CO), ^1H NMR (d-DMSO) δ = 1.462 (s, 9H, $(CH_3)_3$-C), 2.221–2.234 (m, 8H, CH_2CH_2COOPh) 2.261–2.533 (m, 20H, CH_2CONH, CH_2COOPh), 2.461–2.476 (m, 12H, CH_2CH_2N, $CH_2CH_2NH_2$), 2.524–2.611 (m, 12H, CH_2CH_2CONH), 2.720–2.745 (m, 6H, $CH_2N(CH_2)_2$) 3.309–3.342 (m, 10H, CH_2NH_2, $CH_2CH_2N(CH_2)_2$). 6.634 (s, 4H, COCHCO) 7.352–8.112 (b, 24H, Ar-H, Para to Ph-COO and meta to PhCO, ortho to Ph-CO and meta to PhCOO, Para to Ph-CO and meta to PhCO, meta to Ph-COO and Para to PhCO), 8012–8.201 (b, 4H, Ar-H ortho to PhCO), 8.281–8.311 (b, 4H, Ar-H, ortho to PhCOO).

BG3 Yield 74%, IR ν_{max}/cm^{-1}: 1642 (C=O), 1645 (C=O, carboxyl of TPD), 1634 (C=O, B complex with CO), ^1H NMR (d-DMSO) δ = 1.357 (s, 9H, $(CH_3)_3$-C), 1.728 (b, 8H, $CH_2CH_2NH_2$) 2.213-2.709 (t, 28H, CH_2CH_2CO, CH_2CH_2COOPh), 2.444–2.445 (m, 16H, CH_2COOPh), 2.8585 (b, 18H, CH_2CH_2CO, CH_2CH_2N), 3.081 (b, 8H, CH_2CH_2NHCO) 3.3912 (b, 14H, CH_2CH_2N, CH_2CH_2NHCO and CH_2CH_2N [Near focal point]), 6.526 (s, 8H, COCHCO) 7.673–8.033 (b, 48H, Ar-H, Para to Ph-COO and meta to PhCO, ortho to Ph-CO and meta to PhCOO, Para to Ph-CO and meta to PhCO, meta to Ph-COO and Para to PhCO), 8.191 (b, 8H, Ar-H ortho to PhCO), 8.291–8.321 (b, 8H, Ar-H, ortho to PhCOO).

Measuring UV–visible absorption and fluorescence spectroscopy

The TPD-labeled PAMAM Dendrons were dissolved in phosphate buffered saline (PBS) buffer solution, and UV–vis absorption spectra were recorded on a JASCO V-670 spectrophotometer. Emission and excitation spectra were recorded by a HITACHI F-7000 spectrophotometer. To determine the excitation spectrum, all of the TPD-labeled PAMAM dendrons were illuminated at a wavelength ranging from

300 to 900 nm, and the fluorescence was collected at an emission wavelength of 400 nm. To determine the emission spectra, the excitation wavelengths were set to 400 nm, 780 nm, and 860 nm.

Cell culture and treatment

HeLa Cells lines were cultured in DMEM supplemented with 10% FBS in T25 culture flasks and were incubated at 37°C in a humidified atmosphere containing 5% CO_2. Cells were also regularly passaged by trypsinization with 0.1% trypsin in PBS.

Cell affinity experiment of TPD-labeled PAMAM dendrons

The HeLa cells (5×10^5 cells) were cultured on cover slips and kept in a 35 mm Petri dish for 16–20 h. The HeLa was then fixed with 4% paraformaldehyde in PBS for 30 min at room temperature followed by permeabilization in 0.1% Triton X-100 in PBS for 30 min.[20] After rinsing, HeLa cells were incubated with BG1, BG2, and BG3 for 1 h, and the concentration of BG series was fixed at TPD dye at approximately 5 μg/mL. After washing with PBS again, the specimens were stained for lipid droplets by adding 1 μL of dilute Nile red stock solution (1 mg/mL stock solution diluted 1:500 in PBS) for 3 min. Images were obtained using a two-photon Leica TCS SP5 confocal laser microscope (CLSM).

In situ optical monitor uptake process of BG3

HeLa cells (5×10^5 cells) on cover slides after incubation for 24 h were treated with BG3 (TPD dye concentration at 5 μg/ mL in the medium) before observation. BG3 in HeLa was simultaneously observed using a Leica TCS SP5 confocal laser microscope (CLSM) with excitation at 780 and 400 nm and using a filter of 390 nm for BG series detection. To acquire the BG3 uptake in HeLa cells simultaneously, live cells were imaged every 30 s for 18 min at 37°C. The Laser power for two-photon confocal images and one-photon confocal images were both controlled at 6 mW. All settings for observing images from one-photon and two-photon excitation were under identical conditions.

LDH release assay

The effect of the BG3 on the HeLa cell membrane was investigated by a LDH assay after observation by confocal microscopy. The LDH was determined by measuring the fluorescence at 544 nm (excitation)/590 nm (emission) according to manufacturer instructions. The percentage LDH release was calculated using the following formula, where the blank is the fluorescence reading of blank assay solution prepared without the cells. The Laser power for two-photon confocal images and one-photon confocal images were both controlled at 6 mW.

$$\%\text{LDN release} = (\text{experimental value})/(\text{maximal value}) \times 100.$$

Dual imaging of TPD-labeled PAMAM dendrons

HeLa cells (5×10^5 cells) were incubated with BG3 at the dye concentration of 5 μg/mL in the medium; and a Lyso tracker DND 99 subcellular marker was added to the final concentration of 75 nM to monitor the intracellular pathway of BG3. After incubating for 2 h, images were obtained using a two-photon Leica TCS SP5 confocal laser microscope (CLSM).

Co-localization analysis

Co-localization of two image was determined by the ImageJ software (US National Institute of Health) with JACoP plug-in. The confocal image of cell affinity experiment (BG3 in green and Nile Red in red) and dual imaging experiment (BG3 in green and DND99 in red) were analyzed, obtained co-localization value. The plug in provide, Pearson's coefficient (Rr value, ranging between 0 and 1, where 1 is perfect correlation), Manders' overlap coefficient (Ro value, ranging between 0 and 1, where 1 is high and 0 is low co-localization), Manders' colocalization coefficient (M1, fraction of green overlapping red and M2, fraction of red overlapping green), M1 is define as the ratio of the "summed intensities of pixels from green image for which the intensity in the red channel is above zero" to the "total intensity in the green channel" and M2 define conversely for red.

RESULTS AND DISCUSSION

Synthesis and characterization of TPD-labeled PAMAM dendrons

Synthesizing the PAMAM dendrons were initiated from the *N*-boc-ethyldiamine focal point and the dendrons were stretched out by traditional PAMAM branch extension via Michael addition and exhaustive amidation, as shown in Scheme 1(A). To trace the uptake process of a PAMAM dendrons, a marker TPD with two-photon absorption properties was synthesized, as shown in Scheme 1(B). The carboxyl group in TPD was obtained using linker elongation through the ring opening of succinic anhydride. Boron complex in TPD was generated by reacting TPD with $BF_3{\cdot}Et_2O$. Finally, three PAMAM dendrons with different generations conjugating the two-photon dye (BG1, BG2, and BG3) were synthesized by esterification of the PAMAM dendrons (G1, G2, and G3) with TPD, as shown in Scheme 1(C). Successful synthesis of PAMAM dendrons conjugated TPD was confirmed by ^{1}H NMR and GPC. In ^{1}H NMR in d-DMSO, the methyl proton ($CH_2CH_2NH_2$) at 2.8 ppm completely disappeared after TPD esterification of the PAMAM dendrons; however, the benzyl proton of TPD at 6–8 ppm appeared, demonstrating that all primary amines at the periphery of the PAMAM dendrons reacted with TPD. The increase in molecular weight and removal of unreacted monomer were confirmed by GPC. All of the PAMAM dendrons conjugated TPD exhibited a single peak, indicating that purification of PAMAM materials via a dialysis process could be successively achieved, and un-reactants were effectively removed (data not shown). The molecular weight of BG1, BG2, and BG3 were 1000, 2100, and 4600 Da, respectively. Because all the PAMAM dendrons conjugating TPD were readily soluble in a polar solvent (such as methanol, ethanol, or water), it could easily be applied to a biomedical study.

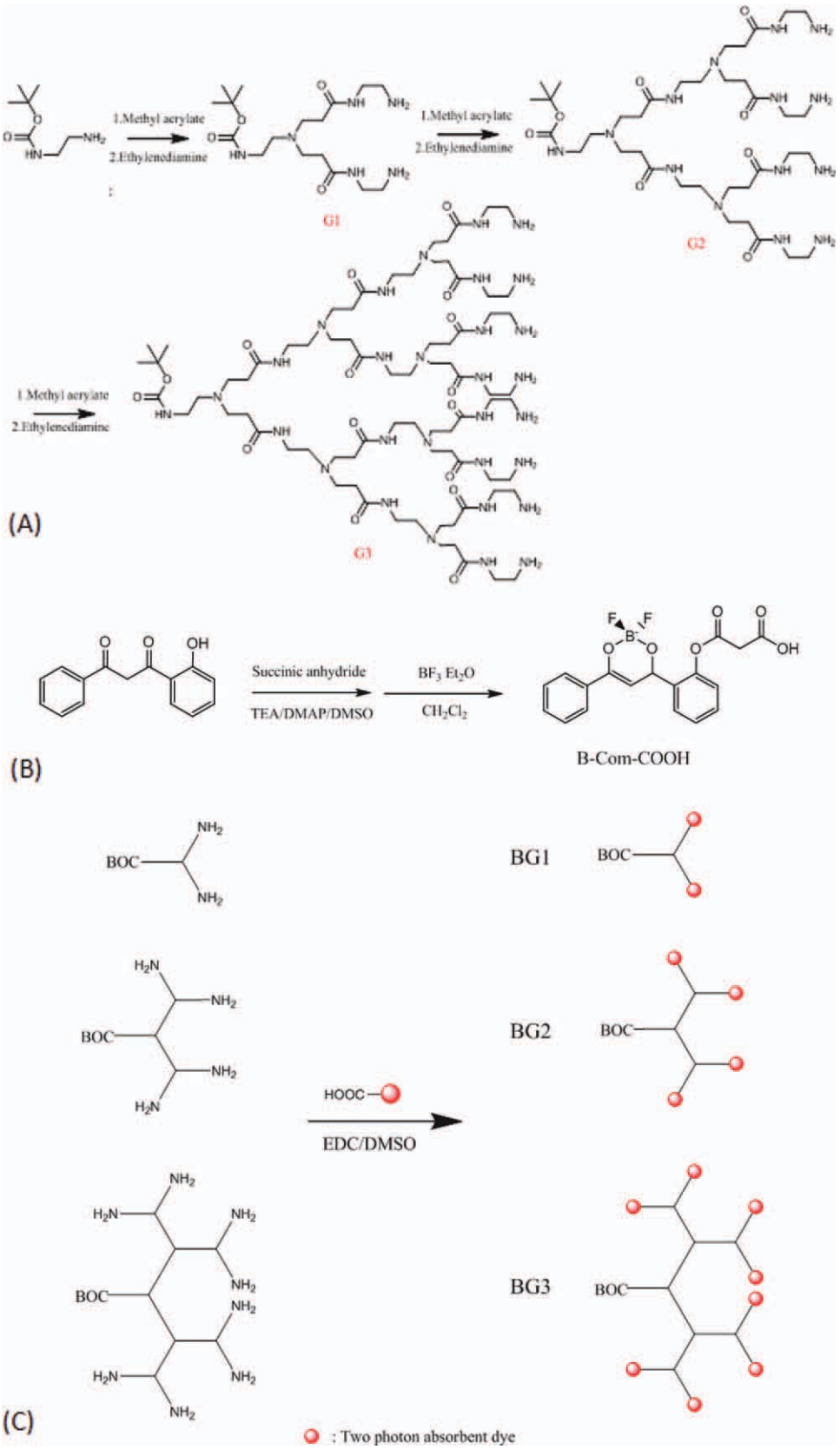

SCHEME 1. (A) Synthesis of PAMAM dendron materials (G1, G2, and G3). (B) Synthesis of two-photon excitation difluoroboron dye (TPD). (C) Synthesis of TPD-labeled PAMAM dendron materials (BG1, BG2, and BG3). [Color figure can be viewed in the online issue, which is available at wileyonlinelibrary.com.]

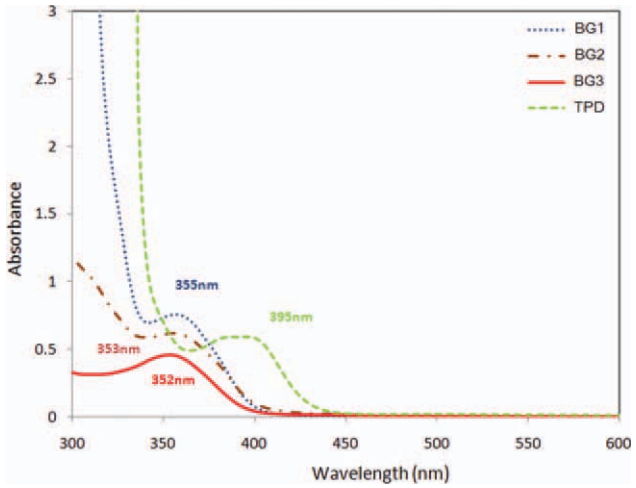

FIGURE 1. The UV–visible spectrum of TPD, BG1, BG2, and BG3 in PBS solution. The concentration of BG series was fixed at 10 mmol of TPD dye in solution. [Color figure can be viewed in the online issue, which is available at wileyonlinelibrary.com.]

UV–vis and fluorescence spectra of TPD-labeled PAMAM dendrons

In the UV–vis spectrum, the two-photon dye dissolved in PBS exhibits an absorption band λ_{max} at 396 nm, as shown in Figure 1. The absorption bands of BG1, BG2, and BG3 exhibit the large blue shift of λ_{max} with generation of dendrons, 357 nm, 355 nm, and 354 nm, respectively. Because the PAMAM dendrons do not absorb in a spectral range at 250–500 nm, this absorption band of BG1, BG2, and BG3 originally comes from the two-photon dye.

The hydrophobic characteristic of the dye moieties mainly drives the aggregation process. H-aggregation of azo-dye or porphyrin within the dendrimers has been reported to be caused mainly by π–π stacking of the molecule.[21] Dye molecules are known to form aggregates in the presence of anionic and cationic polyelectrolytes.[22–25] The polyelectrolyte chains of PAMAM dendrons also provide an electrostatic scaffold that assists aggregation among dye molecules by partly neutralizing the coulombic repulsions.[26] That might be a reason why H-aggregation increased with increased dendron generation.

The emission spectra at 500 nm of TPD, BG1, BG2, and BG3 show common excitation bands at 780 nm, 810 nm, and 860 nm, as shown in Figure 2. The excitation band at 810 nm showing two times the absorption band of TPD could be classified as a two-photon absorption of energy for electronic (S0 → S1) transition; and the band obtained at 780 nm corresponds to higher energy for electronic (S0 → SN) transition. The excitation band at 860 nm might come from multi-photon absorption of TPD. These electronic transitions are schematically indicated in the insert picture of Figure 2. Multi-bands of the TPD and TPD conjugated dendrons in the near infrared region could be widely applied to cell bio-imaging. Fluorescence only occurs in the S0 state, even if emission photons differ significantly in energy. In nonlinear optical fields and applications, the linear and nonlinear photophysical properties of TPD are crucial when investigating specific fluorescence characteristics. Therefore, the following experiment emphasizes the two-photon fluorescence of TPD-labeled PAMAM dendrons activated at 780 nm, which also refers to the near infrared region.

Figure 3 shows the two-photon excitation fluorescence of BG1, BG2, and BG3 in PBS. Findings show the same blue shift behavior when incorporating the TPD in the dendrons periphery. The λ_{max} in the photon excitation profile (one-photon and multi-photon are shown in Supporting Information) behaves as a small blue shift relative to the UV–vis absorption spectrum in Figure 1. This difference in blue shift may arise from a transition symmetric requirement for two-photon excitation and three-photon excitation profiles of TPD dye in vibration transition.[27] The fluorescence

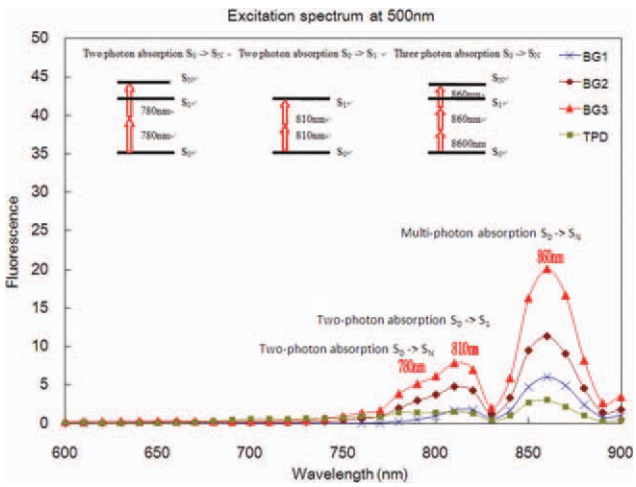

FIGURE 2. Fluorescence excitation spectrum of TPD, BG1, BG2, and BG3 in PBS solution fixed the emission peak at 500 nm. The Jablonski diagrams for the electronic transitions were inserted in the figure. The concentration of BG series was fixed at 10 mmol of TPD dye in solution. [Color figure can be viewed in the online issue, which is available at wileyonlinelibrary.com.]

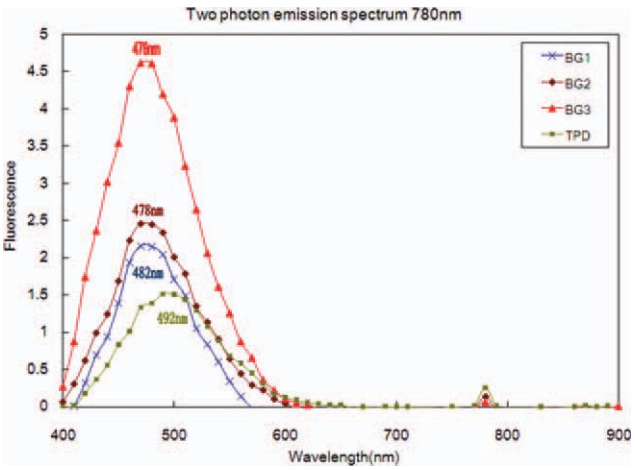

FIGURE 3. Two-photon emission spectrum of TPD, BG1, BG2, and BG3 in PBS excited at 780 nm. The concentration of BG series was fixed at 10 mmol of TPD dye in solution. [Color figure can be viewed in the online issue, which is available at wileyonlinelibrary.com.]

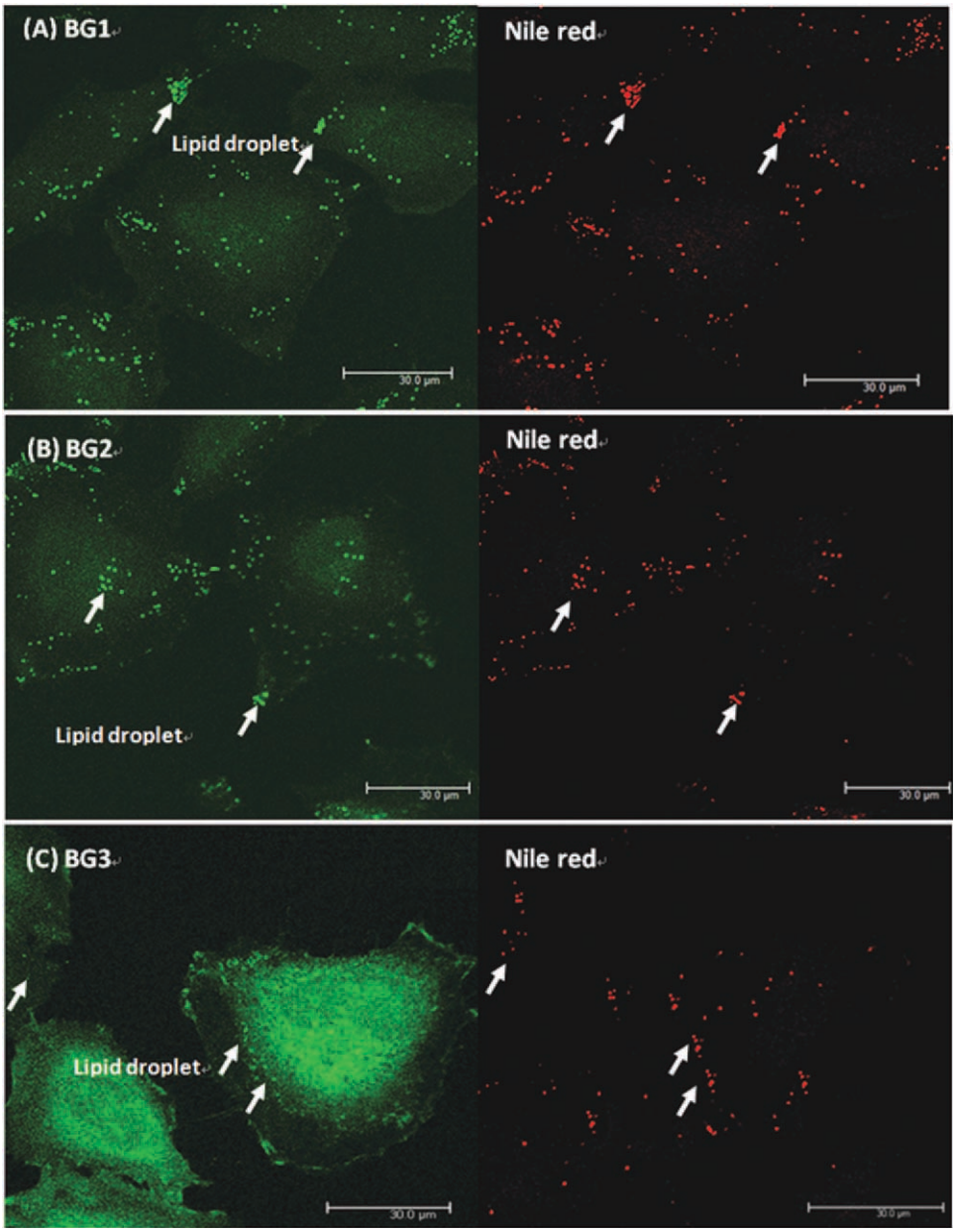

FIGURE 4. Two-photon confocal image of BG1, BG2, and BG3 incubated with fixation HeLa cells for 30 min. HeLa cells were extracted with 0.1% Triton X-100 for 30 min after fixation. [Color figure can be viewed in the online issue, which is available at wileyonlinelibrary.com.]

intensity of one-photon excitation for BG2 and BG3 appeared to be the same (see Supporting Information S1). However, the intensity at the multiphoton excitation profile is dramatically different (as seen in Figs. 3, S2, and S3), which show the multi-photon emission spectrum of the BG series. Therefore, combining the multiphoton absorption dye in the dendrons could enhance fluorescence intensity for optical imaging research.

Cell affinity study of TPD-labeled PAMAM dendrons

To visualize the physical interaction between the TPD-labeled PAMAM dendrons and HeLa cells, this study investigated the affinity of TPD-labeled PAMAM dendrons within HeLa cells in the internalization process. This work examined the dendrons in dead cells, because live cells contain a complicated biological uptake process, making it difficult to estimate the affinity of the TPD-labeled PAMAM dendrons with cells. Triton X-100 is one of the most widely used non-ionic surfactants for lysing cells to extract protein and other cellular organelles or to permeabilize the cell membrane.[28–30] Thus, the fixed HeLa cells were immersed in 0.1% Triton X-100 for 30 min to increase permeability of dendron materials through the cell membrane. It has been reported that the permeability of cells could be enhanced when increasing exposure time with Triton x-100.[31] In Figure 4(A,B), fluorescence light of aggregates in a spherical shape was observed for HeLa incubated with BG1 and BG2. The fluorescence appearing in the organelle might be from the diffusion of

TABLE I. Co-localization Coefficients Obtained by Computational Analysis of Confocal Image (Figs. 4 and 7)

			Co-localization Coefficient			
	1 (Green)	2 (Red)	Rr	Ro	M1	M2
Cell affinity experiment	BG1	Nile red	0.863	0.999	0.969	0.822
	BG2	Nile red	0.924	0.999	0.973	0.900
	BG3	Nile red	0.609	0.996	0.333	0.919
Dual image experiment	BG3	DND99	0.800	0.930	0.520	0.873

Definition of coefficients was described in the experimental section.

TPD-labeled PAMAM dendrons driven by a concentration gradient and a high concentration of TPD-labeled PAMAM dendrons in medium diffuse to low concentration of cells. Figure 4(C) shows the remarkable results obtained from the HeLa cells incubated with BG3. We still can find spherical fluorescence dots within cells, with the most crucial being the fluorescence spread on the whole cell's membrane, when compared with BG1 and BG2.

In Figure 4(A,B), the fluorescent spherical dots in the cells overlap with lipid droplet organisms within the cells. Lipid droplets are spherical organelles ranging in diameter from 50 nm at formation to 200 μm in mature adipocytes. In addition, lipid droplets (LDs) are cytoplasmic organelles found in most cell types, consisting of two major compartments: a core filled with neutral lipids, such as triacylglycerides, diacylglycerol, and cholesterol esters; and a surrounding phospholipid monolayer, containing free cholesterol and proteins.[32] Amphiphilic BG series can be dissolved not only in the water phase, but also in the organic phase. All BG series should have the possibility of accumulating in those hydrophobic nanopools of lipid droplets. The high intensity of fluorescence spread on the whole cell's membrane incubated with BG3 demonstrates the third generation TPD-labeled PAMAM dendron's high affinity on the cell membrane. Although the fluorescence spread on the whole cell, as shown in Figure 4(A,B), we can conclude that Generation 3 dendron materials exhibited higher multivalency behavior than did Generations 2 and 1. This result indicates that Generation 3 dendrons can act as dendrimers to achieve the multivalency function on cell membranes.

To reveal the presence and distribution of areas of co-localization of TPD-labeled dendrons materials and lipid droplet in HeLa cells, we analyze two image (BG series in green and Nile red in red) using ImageJ for Figure 4(A–C). Four colocalization coefficients were calculated, such as Pearson's correlation coefficient (Pr),[33] Manders' overlap coefficient (Po),[33] and colocalization coefficient (M1 and M2)[34] are presented in Table I. For the HeLa cells co-culture with BG1, the small area of co-localization of BG1 and Nile red were characterized and exhibited high correlation indicated by Pr = 0.863, Ro = 0.999, M1 = 0.969, and M2 = 0.822. Also, in the case of HeLa cells co-culture with BG2 the co-localization of BG2 and Nile red were very high (Pr = 0.924, Ro = 0.999, M1 = 0.973, and M2 = 0.900), and therefore we can conclude that both BG1 and BG2 exhibit high co-localization with lipid droplet in the HeLa cells. However, HeLa cells cultured with BG3 showed a different pattern, lower Pearsons' correlation coefficient and M1 coefficient were found (Pr = 0.609 and M1 = 0.333). These results suggest that the interaction between the cell membrane and BG3 diminished the Pr and M1 coefficient value. In contrast, the Manders' overlap coefficient (Po = 0.996) and co-localization coefficient (M2 = 0.919) of BG3 were similar with the result in BG1 and BG2 reveal that high degree of Nile red overlap with BG3 within the cells.

Uptake behavior of TPD-labeled PAMAM dendrons *in situ*

High generation TPD-labeled PAMAM dendrons (BG3) were incubated with the living HeLa cells for observing the cell uptake process of dendrons *in situ*, as shown in Figure 5. The emission spectrum of BG3 within HeLa cells is the same as BG3 in the PBS excited 780 nm (see Supporting Information Fig. S4). In the early stage of incubation shown in Figure 5(A,B), fluorescent small spots appeared within the cells, indicating that the TPD-labeled PAMAM dendrons travel through the endocytosis pathway. A living image was taken every 30 s during the cell uptake process of the TPD-labeled PAMAM dendrons. First, shirking HeLa cells [appearing in Fig. 5(C)] and floating HeLa cells [appearing in Fig. 5(D)] indicate that the two-photon light triggers the cells entering the apoptotic pathway. Second, a fluorescence trace of outflow from the cell membrane in Figure 5(E,F) reveals that the cell membrane was damaged. Both of these effects on the cell reveal that phototoxicity of TPD conjugated PAMAM dendrons, excited by the two-photon laser, damaged the cell membrane. Two-photon excitation of TPD can be concentrated to a small volume at the laser focus; therefore, two-photon activated phototoxicity could be strengthened at the region where TPD is located.[35,36] Phototoxicity is strongly dependent on two factors: laser power and the dosage of dye (photosensitive agent) because the laser power used in confocal microscopy is set to 6 mW and is quite low. The phototoxicity might be caused by the binding of a large quantity of TPD-labeled PAMAM dendrons on the membrane during the uptake process. To distinguish the two-photon effects of the TPD-labeled PAMAM dendrons influencing the cell membrane, the research was also performed by one-photon excitation with HeLa cells incubated with the TPD-labeled PAMAM dendrons. This condition proves that no membrane damage or floating cells occurred (see Supporting Information Fig. S5). In addition, the same condition

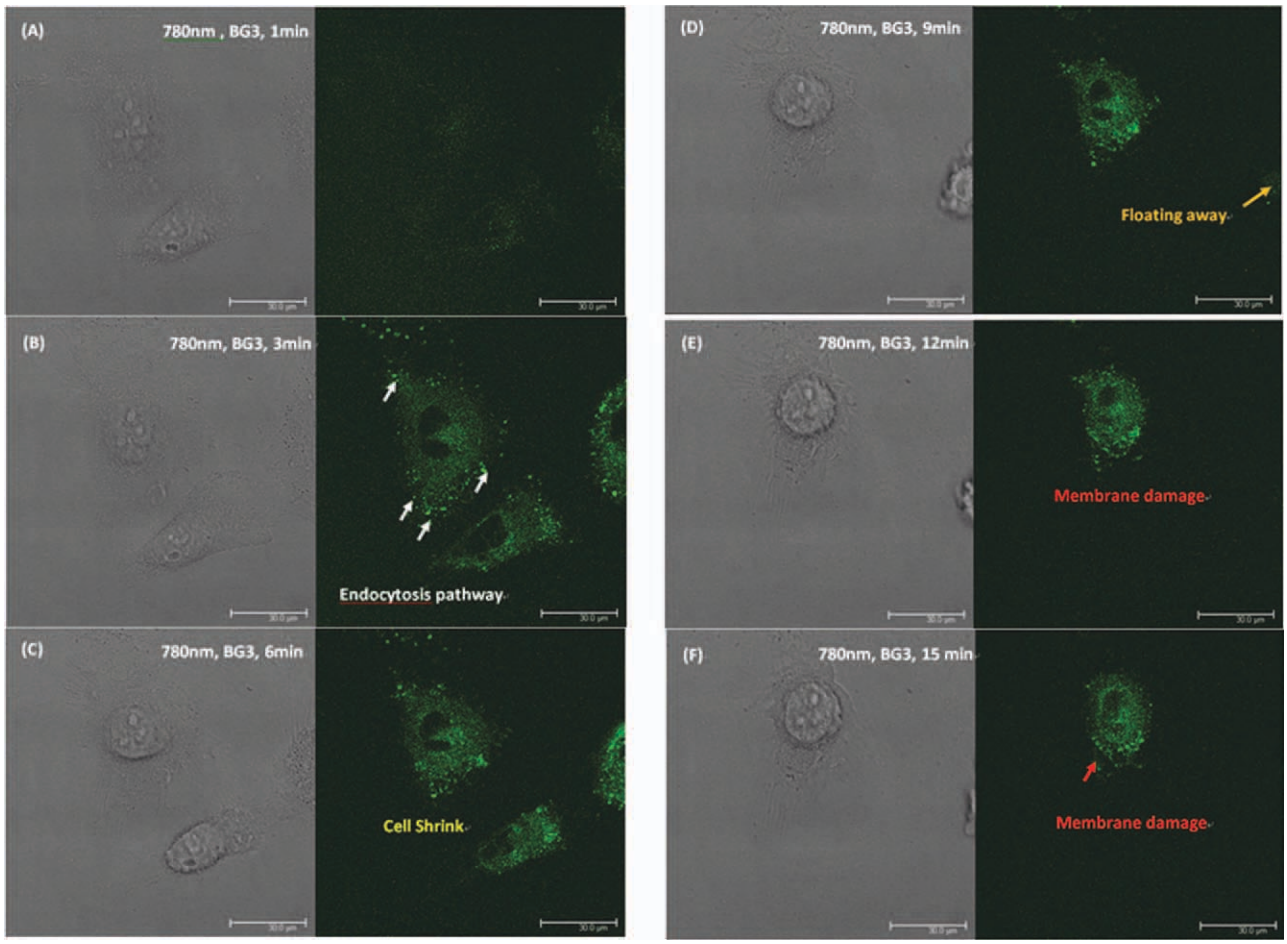

FIGURE 5. *In situ* two-photon optical image of cell uptake process of BG3 incubated with living HeLa cells at different time lapses. A: 1 min; B: 3 min; C: 6 min; D: 9 min; E: 12 min; and F: 15 min. [Color figure can be viewed in the online issue, which is available at wileyonlinelibrary.com.]

for live confocal images was performed, and no floating cell/membrane damage for either one-photon or two-photon excitation occurred, without adding BG3 (see Supporting Information Figs. S6 and S7). To further prove that the cell membrane damage occurred after two-photon light treatment, the integrity of the plasma membrane was evaluated by an LDH assay after light treatment. As shown in Figure 6, this result confirms that BG3 did not cause cell membrane damage after one-photon irradiation. The LDH release showed a time dependent on the two-photon light treatment, 25.78% of LDH release was obtained at 12 min after two-photon confocal microscopy observation. The release of LDH in the cytotoxicity results is consistent with the membrane damage found in the confocal microscopy image. Therefore, membrane damage or disruption of cell membranes can be ascribed to a concentrated photo-reaction effect on cell membranes from the following: (1) the multivalency binding effect of BG3, leading to a large quantity of two-photon dye localized on the membrane during the uptake process; and (2) the two-photon excitation that occurred on the focal region. The subcellular localization of photosensitizers has been shown to be a key factor in photodynamic treatment inducing cell death.

Dual labeling imaging of TPD-labeled PAMAM dendrons

Lysotraker red DND 99, one of the two-photon fluorescence probes for imaging acidic vesicles in live cells, was used for dual imaging in this study. Figure 7 shows the fluorescent image of BG3 after incubation with HeLa cells stained with

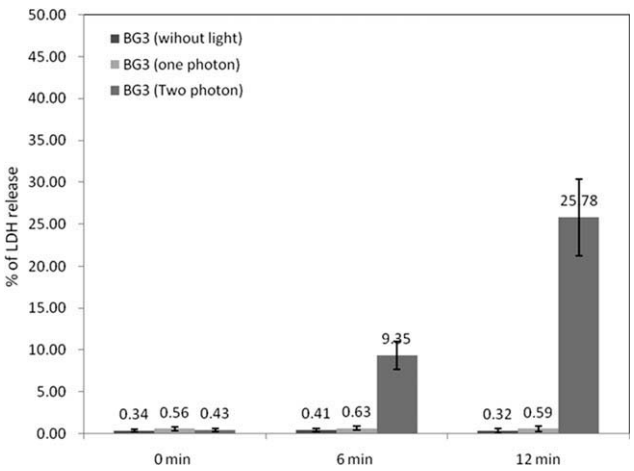

FIGURE 6. Percentage of total LDH release from HeLa cells.

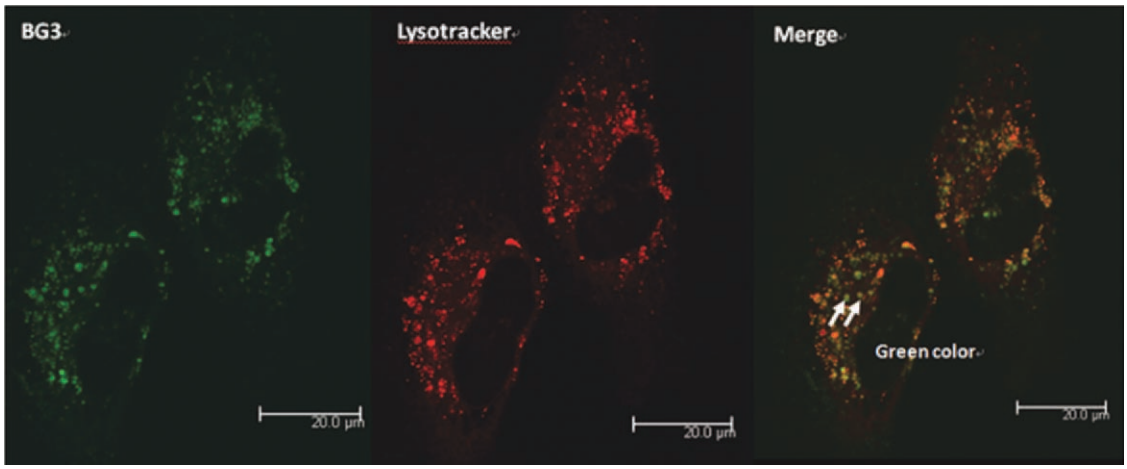

FIGURE 7. Evaluation of cell uptake of BG3 with living HeLa cells for 2 h; the green color represents BG3 dendron materials, and the red color represents the cytosome compartment. [Color figure can be viewed in the online issue, which is available at wileyonlinelibrary.com.]

DND99 for 2 h at 37°C. When the excitation laser is tuned to 780 nm, it should be excited with both BG3 and DND99, and the band path filters should facilitate detecting two separate emissions simultaneously. To quantify the co-localization of BG3 and DND99 in the HeLa cells, Figure 7 was also analyzed by imageJ with JACOP plug in. The co-localization coefficients were calculated in Table I. The high value of Pearson's correlation coefficient (Pr = 0.800), Manders' overlap coefficient (Po = 0.930) and M2 (M2 = 0.873) revealed that the highest degree of red color (DND99) co-localized with the green color of BG3. In contrast, the low value of M1 (M1 = 0.520) demonstrated only 52% of green color colocalized with red color. This result showed that the endocytosis is not the only way for BG3 internalized into the HeLa cells.

The ability of dendrimers to cross cell membranes is of much interest because of their application in drug and gene delivery. Endocytosis of the TPD-labeled PAMAM dendrons should be located at the lysosome, which we stained with DND 99 to develop a red color. Otherwise, the dendrimers penetrate the cell membrane, re-arrange lipid bilayers via hole-formation, and enter the cells. Although we cannot directly observe the holes exhibition on cells membrane from confocal microscopy image, the accumulation of BG3 did not match lysosome indicates the possibility of BG3 crossing the cell membrane and located within others organelles. This may be why green fluorescence shows more spots than red one in the merged figure (the arrow part). Although several studies on dendrimer and liposome interaction have revealed structural changes to the lipid bilayer,[37–41] the current study provides different evidence that TPD-labeled PAMAM dendron crossed the cell membrane and accumulated on the organelle, using dual imaging from two-photon confocal microscopy.

CONCLUSION

This study developed a two-photon difluoroboron dye and the multi-emission band of TPD extends the usage of a light source in the near infrared region. The multiple TPD ligands conjugated in BG3 achieved the chelating effect of dendrimer on cell membranes[42] which was confirmed in the cell affinity experiment. Previous reports have indicated that the dendrimer uptake process results in membrane absorption and subsequent endocytosis.[39] Photo-damage on the cell membrane during live cell optical imaging, when HeLa cells were incubated with BG3, also indicated a high possibility of TPD-labeled PAMAM dendrons binding on the cell membrane during the uptake process. Emission bands at long wavelengths on the spectrum of TPD-labeled PAMAM dendrons eventually facilitated dual image observation with the cell simultaneously stained with DND-99. These findings not only provide useful information for designing the TPD-labeled PAMAM dendrons as macromolecular probe in drug or gene carrier, but also establish a new two-photon difluoroboron dye for biomedical applications.

ACKNOWLEDGMENTS

The authors thank the National Science Council of the Republic of China, Taiwan, for financially supporting this work (NSC 99-2218-E-011-007, NSC 99-2923-M-011-001-MY3, and 98WFA2500198). Financial support from Formosa Program (Grant 2009TW0031) and the Scientific-Technical Services of University of Barcelona (Dr. Maria Calvo) for cell affinity experiments are also acknowledged.

REFERENCES

1. Chow YL, Johansson CI, Zhang YH, Gautron R, Yang L, Rassat A, Yang SZ. Spectroscopic and electrochemical properties of 1,3-diketonatoboron derivatives. J Phys Org Chem 1996;9:7–16.
2. Zhang G, Chen J, Payne SJ, Kooi ST, Demas JN, Fraser CL. Multi-emissive difluoroboron dibenzoylmethane polylactide exhibiting intense fluorescence and oxygen-sensitive room temperature phosphorescence. J Am Chem Soc 2007;129:8942–8943.
3. Loudet A, Burgess K. BODIPY dyes and their derivatives: Syntheses and spectroscopic properties. Chem Rev 2007;107:4891–4832.
4. Zheng Q, He GS, Prasad PN. A novel near IR two-photon absorbing chromophore: Optical limiting and stabilization performances at an optical communication wavelength. Chem Phys Lett 2009; 475:250–255.
5. Voit B. New developments in hyperbranched polymers. J Polym Sci Part A: Polym Chem 2000;38:2505–2525.

6. Lee CC, Mackay AJ, Frechet JMJ, Szoka FC. Designing dendrimer for biological application. Nat Biotechnol 2005;23:1517–1526.
7. Al-Jamal KT, Ramaswamy C, Florence AT. Supramolecular structure from dendrons and dendrimers. Adv Drug Delivery Rev 2005; 57:2238–2270
8. Amir JR, Pessah N, Shamis M, Shabat D. Self-immolative dendrimers. Angew Chem Int Ed 2003;42:4494–4499.
9. Shum P, Kim JM, Thompson DH. Phototriggering of liposomal drug delivery systems. Adv Drug Delivery Rev 2001;53:273–284.
10. Szalai ML, Kevwitch RM, McGrath DV. Geometric disassembly of dendrimers: Dendritic amplification. J Am Chem Soc 2003;125: 15688–15689.
11. de-Groot FMH, Albrecht C, Koekkoek R, Beusker HP, Scheeren HW. Cascade-release dendrimers liberate all end groups upon a single triggering event in the dendritic core. Angew Chem Int Ed 2003;42:4490–4494.
12. Parimi S, Timothy BJ, Callen FD, Prestidge CA. Mechanistic insight into cell growth, internalization and cytotoxicity of PAMAM dendrimers. Biomacromolecules 2010;11:382–389.
13. Zhang YZ, Smith BD. High-generation polycationic dendrimers are unusually effective at disrupting anionic vesicles: Membrane bending model. Bioconjug Chem 2000;11:805–814.
14. Uppuluri S, Piehler L, Li J, Hagnauer LG, Tomalia DA. Core–shell Tecto(dendrimers): Synthesis and characterization of saturated shell models. Adv Mater 2000;12:796–800.
15. Mecke A, Uppuluri S, Sassanella TM, Lee DK, Ramamoorthy A, Baker JR, Orr GB, Banaszak MM. Holl. direct observation of lipid bilayer disruption by poly(amidoamine) dendrimers. Chem Phys Lipids 2004;132:3–14.
16. Leroueil RP, Berry AS, Duthie K, Han G, Rotello MV, McNerny QD, Baker R, Orr G, Holl B. Wide varieties of cationic nanoparticles induce defects in supported lipid bilayers. Nano Lett 2008;8: 420–424
17. Hong S, Bielinska U, Mecke A, Keszler B, Beals L, Shi X, Balogh L, Orr GB, Baker RJ, Banaszak MM, Holl B. Interaction of poly(amidoamine) dendrimers with supported lipid bilayers and cells: Hole formation and the relation to transport. Bioconjug Chem 2004;15: 774–782.
18. Hong S, Leroueil RP, Janus KE, Peters LJ, Kober MM, Islam TM, Orr GB, Baker RJ, Holl MMB. Interaction of polycationic polymers with supported lipid bilayers and cells: Nanoscale hole formation and enhanced membrane permeability. Bioconjug Chem 2006;17: 728–734.
19. Mullen GD, Fang M, Desai A, Baker JR, Orr GB, Holl MMB. A quantitative assessment of nanoparticle ligand distributions: Implications for targeted drug and imaging delivery in dendrimer conjugates. ACS Nano 2010;4:657–670.
20. Koley D, Bard AJ. Triton X-100 concentration effects on membrane permeability of single HeLa cells by scanning electrochemical microscopy (SECM). Proc Natl Acad Sci USA 107:16783–13787.
21. Hunter AC, Sander JKM. The nature of pi-pi interaction. J Am Chem Soc 1990;112:5525–5534.
22. Wiwattanapatapee R, Carreno-Gomez B, Malik N, Duncan R. Anionic PAMAM dendrimers rapidly cross adult rat intestine *in vitro*: A potential oral delivery system?Pharm Res 2000;17:991–998.
23. Paulo RMP, Costa SMB. Non-covalent dendrimer-porphyrin interactions: The intermediacy of H-aggregates. Photochem Photobiol Sci 2003;2:597–604.
24. Shcharbin D, Klajnert B, Mazhul V, Bryszewska M. Dendrimer interactions with hydrophobic fluorescent probes and human serum albumin. J Fluorescence 2005;15:21–28.
25. Karukstis KK, Perelman LA, Wong WK. Spectroscopic characterization of azo dye aggregation on dendrimer surface. Langmuir 2002;18:10363–10371.
26. Kubat P, Lang K, Janda P, Anzenbacher P. Interaction of porphyrins with a dendrimer template self-aggregation controlled by pH. Langmuir 2005;21:9714–9720.
27. Samoc M, Morrall PJ, Dalton TG, Marie PC, Humphery MG. Two photon and three photon absorption in organometallic dendrimer. Angew Chem 2007;46:731–733.
28. Gennuso F, Fernetti C, Tirolo C, Testa N, L'Episcopo F, Caniglia S, Morale CM, Ostrow DJ, Pascolo L, Tiribelli C, Marchetti B. Bilirubin protects astrocytes from its own toxicity by inducing up-regulation and translocation of multidrug resistance-associated protein 1 (mrp1). Proc Natl Acad Sci USA 2004;101:2470–2475.
29. Rajagopal A, Pant C, Simon M, Chen Y. *In vivo* analysis of human multidrug resistance protein (MRP1) activity using transient expression of fluorescently Tagged MRP1. Cancer Res 2002;62: 391–396.
30. Hipfner RD, Gauldie DS, Deeley GR, Cole SPC. Detection of the Mr 190,000 multidrug resistance protein, MRP, with monoclonal antibodies. Cancer Res 1994;54:5788–5792.
31. Koley D, Bard AJ. Triton X-100 concentration effects on membrane permeability of single HeLa cells by scanning electrochemical microscopy (SECM). Proc Natl Acad Sci USA 107:16783–13787.
32. Murphy DJ. The biogenesis and functions of lipid bodies in animals, plants and microorganisms. Prog Lipid Res 2001;40: 325–438.
33. Manders MME, Verbeek JF, Aten JA. Measurement of co-localization of objects in dual-color confocal images. J Microsc 1993;169: 375–382.
34. Manders MME, Stap J, Brakenhoff JG, van Driel R, Aten JA. Dynamics of three-dimensional replication patterns during the Sphase, analysed by double labelling of DNA and confocal microscopy. J Cell Sci 1992;103:857–862.
35. Dahlstedt E, Collins AH, Balaz M, Kuimova KM, Khurana M, Wilson CB, Phillips D, Anderson HL. One- and two-photon activated phototoxicity of conjugated porphyrin dimers with high two-photon absorption cross sections. Org Biomol Chem 2009;7:897–904.
36. Starkey RJ, Rebane KA, Drobizhev AM, Meng F, Gong A, Elliott A, Mcinnerney K, Spangler CW. New two photon activated photodynamic therapy sensitizers induce xenograft tumor regression after near ir laser treatment through the body if the host mouse. Clin Cancer Res 2008;14:6564–6573.
37. Saovapakhiran A, D'Emanuele A, Attwood D, Penny J. Surface modification of PAMAM dendrimers modulates the mechanism of cellular internalization. Bioconjug Chem 2009;20:693–701.
38. Ottaviani FM, Daddi R, Brustolon M, Turro JN, Tomalia DA. Structural modifications of DMPC vesicles upon Interaction with poly (amidoamine) dendrimers studied by CW-electron paramagnetic resonance and electron spin-echo techniques. Langmuir 1999;15: 1973–1980.
39. Zhang YZ, Smith BD. High-generation polycationic dendrimers are unusually effective at disrupting anionic vesicles: Membrane bending model. Bioconjug Chem 2000;11:805–814.
40. Karoonuthaisiri N, Titiyevskiy K, Thomas JL. Destabilization of fatty acid-containing liposomes by. polyamidoamine dendrimers. Colloids Surf B 2003;27:365–375.
41. Sideratou Z, Foundis J, Tsiourvas D, Nezis PI, Papadimas G, Paleos CM. A novel dendrimeric "glue" for adhesion of phosphatidyl choline-based liposomes. Langmuir 2002;18:5036–5039.
42. Mammen M, Choi KS, Whitesides GM. Polyvalent interactions in biological systems: implications for design and use of multivalent ligands and inhibitors. Angew Chem Int Ed 1998;37:2754–2799.